



**Phase separation of the electron-ion conducting layer on the surface of  $\text{TiP}_2\text{O}_7$ , anode material for aqueous lithium rechargeable batteries**

Journal:	<i>Journal of Materials Chemistry A</i>
Manuscript ID	TA-COM-02-2016-001291.R2
Article Type:	Communication
Date Submitted by the Author:	11-Jul-2016
Complete List of Authors:	Zhang, Hanping; Changzhou university, Zhou, Yisen; Changzhou University, Li, Chenggang; Changzhou University, Yang, Chao; Changzhou University, Zhu, Tian; Changzhou University,



Journal Name

COMMUNICATION

## Phase separation of the electron-ion conducting layer on the surface of $\text{TiP}_2\text{O}_7$ anode material for aqueous lithium rechargeable batteries †

Received 00th January 20xx,  
Accepted 00th January 20xx

DOI: 10.1039/x0xx00000x

Hanping Zhang,\* Yisen Zhou,<sup>†</sup> Chenggang Li,<sup>†</sup> Chao Yang and Tian Zhu

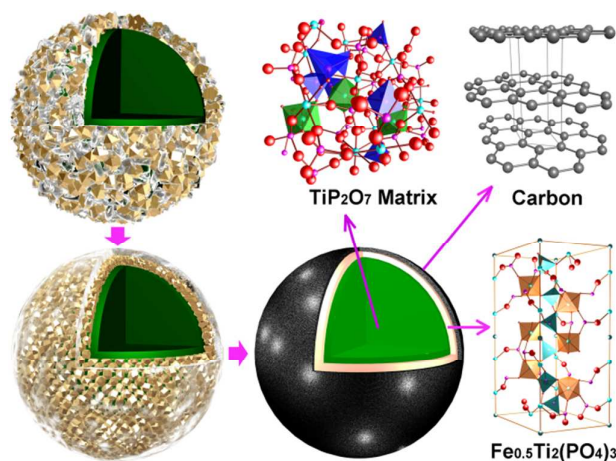
www.rsc.org/

**A phase separation of carbon and  $\text{Fe}_{0.5}\text{Ti}_2(\text{PO}_4)_3$  bi-layer was fabricated on the surface of  $\text{TiP}_2\text{O}_7$  particles. As the carbon layer improves the electronic conductivity, and the  $\text{Fe}_{0.5}\text{Ti}_2(\text{PO}_4)_3$  layer favors the transference of lithium ions, the capacity and rate performance of the  $\text{TiP}_2\text{O}_7$  anode material for aqueous lithium rechargeable batteries are greatly enhanced.**

We are making poor use of energy to support modern living. From eons ago to now, burning something (including burning gasoline in a car) has been an important strategy to get energy. A key drawback is that the efficiency of combustion is limited by a Carnot heat engine to a very low level, emitting greenhouse gases at the same time. The battery is a type of clean and high-efficiency power source converting chemical energy directly into electricity. Batteries overtaking gasoline on a large scale, especially in vehicles, would mark true technological progress. Subjected to the poor performance of electrode materials, however, the chemical battery is currently nowhere near as powerful as fossil fuels.<sup>1,2</sup> The lithium ion battery, for example, one of the most advanced power sources, suffers from its key electrode materials, whether anode or cathode.<sup>3–8</sup> Oxides (such as SnO and  $\text{TiO}_2$ ),<sup>9,10</sup> composite oxides (such as  $\text{LiCoO}_2$ ,  $\text{LiMn}_2\text{O}_4$  and  $\text{TiP}_2\text{O}_7$ ),<sup>11–13</sup> and complex anionic compounds (such as  $\text{LiFePO}_4$  and  $\text{LiFeSO}_4\text{F}$ ) are semiconductors or even nonconductors.<sup>14–16</sup> As a result, the rate at which the current flows is low, and the power of the battery is far inferior to that of a combustion engine. To enhance the power of the battery, choices come down to elevating the rate performance of anode and cathode materials. Two strategies have obtained great success: carbon-coating to improve the mobility of electrons and nano-sizing to reduce the diffusive distances of electrons and lithium ions.<sup>17,18</sup> Carbon-coating is especially successful in the modification of  $\text{LiFePO}_4$  cathode material that was a nonconductor and now is commercially available.<sup>19,20</sup>

The fact that electrochemical performance such as charge-discharge rate and capacity can be elevated singly by carbon-coating is surprising. Firstly, carbon-coating enhances the electronic conductivity on the surface rather than in the matrix

of a particle, which would indicate that, compared with the bulk of the material particle, the electronic conductivity between particles has greater impact on the performance of the material. Secondly, as is well known, lithium ions would simultaneously move in or out the electrode matrix along with the electrons, which means the mobility of lithium ions between particles has also an important influence on the performance of the material.<sup>21,22</sup> Therefore, there is a logical possibility that elevating the mobility of lithium ions might deliver an added bonus. After all, lithium ions are much larger than electrons, and have to overcome more resistance to move under the same electric field. In 2009, Cedar et al. reported that the modification of  $\text{LiFePO}_4$  through controlled off-stoichiometry can extremely improve the rate performance equivalent to a full battery discharging in 10–20 S.<sup>23</sup> They ascribed the result to the creation of a fast ion-conducting surface phase. Unfortunately, their result had been plunged into a bitter dispute.<sup>24,25</sup> Until now, the shell in a core-shell structure is still studied in view as a protective surface layer rather than an ionic conductor even though the charge transfer resistance ( $R_{ct}$ ) of the modified host is much lower than expected from the beginning to the extended cycling.<sup>26</sup> Recently, the study of using  $\text{Li}_2\text{TiO}_3$ , a  $\text{Li}^+$ -conductive nano material, to cover on the  $\text{LiMO}_2$  ( $M = \text{Ni}, \text{Co}, \text{Mn}$ ) nanobelts has got a positive result,<sup>27</sup> which facilitates us to re-evaluate the effect of coating. Since the transference of ions is usually accompanied with electrons, we believe that a phase separated bi-layer for conducting electrons and ions respectively might get better result. In this study, we successfully fabricated a phase separation of an electron-ion conducting layer on the surface of  $\text{TiP}_2\text{O}_7$  anode material for an aqueous lithium battery. As a result, not only the rate performance, but also the capacity is notably improved. Of course, protection for the material against the attack from the electrolyte would also be reinforced, especially for aqueous solutions which are more corrosive than organic solutions. Here, the safety advantages of aqueous solutions should be addressed for lithium batteries used to drive vehicles.



Scheme 1 Schematic fabrication process of the electron-ion phase-separated conductor on the surface of the  $\text{TiP}_2\text{O}_7$  matrix.

At a low cost,  $\text{TiP}_2\text{O}_7$  is easily prepared at a low temperature in air. As an anode material, compared with  $\text{Li}_4\text{Ti}_5\text{O}_{12}$ ,<sup>28,29</sup>  $\text{TiP}_2\text{O}_7$  would be cheap since it contains no lithium. However,  $\text{TiP}_2\text{O}_7$  has long been obviated from the list of candidates of anode materials, especially in aqueous electrolyte since capacity is low and cycling performance is poor, not to mention its terrible rate performance.<sup>30</sup> Modification with doping in the crystal lattice has been of little help since the matrix of  $\text{TiP}_2\text{O}_7$  is stable and has a 2D lithium ion diffusion path with good lithium conductivity itself.<sup>31,32</sup> It is thereby reasonable to enhance its capability by improving the electronic conductivity. However, the application of surface modification or particle downsizing fails to improve its capacity above  $100 \text{ mA h g}^{-1}$ , a commercial value in both non-aqueous and aqueous electrolytes.<sup>33–35</sup> By constructing a carbon- $\text{Fe}_{0.5}\text{Ti}_2(\text{PO}_4)_3$  (ITP) phase separated conducting layer on the surface of the matrix, we successfully elevate the capacity to  $115 \text{ mA h g}^{-1}$  with the mass of the conducting bi-layer being reckoned in. Here carbon acts as the electron conductor, and ITP as the ion conductive layer, which has been confirmed to be a fast ionic conductor.<sup>36</sup>

The phase separating process is illustrated in Scheme 1. To fabricate the double layer conductor, the bared  $\text{TiP}_2\text{O}_7$  particles are firstly prepared in air according to versions of previously published methods.<sup>37</sup> Afterwards, sucrose and the precursor of ionic conductor,  $\text{FeC}_2\text{O}_4$ , are mixed and evenly spread on the surface of the  $\text{TiP}_2\text{O}_7$  host. When heated in nitrogen flow, the precursor reacts with the matrix to form the inner ITP layer, at the same time, the melted sucrose is pushed out by the reaction between the precursor and the matrix, and eventually carbonized to become the outer electronic conductive layer. As a result, the phase separation between the ionic conductive layer and the electronic conductive layer occurs. In comparison, a carbon mono-layer and an ITP mono-layer is prepared on the surface of  $\text{TiP}_2\text{O}_7$  particle under the same conditions, respectively.

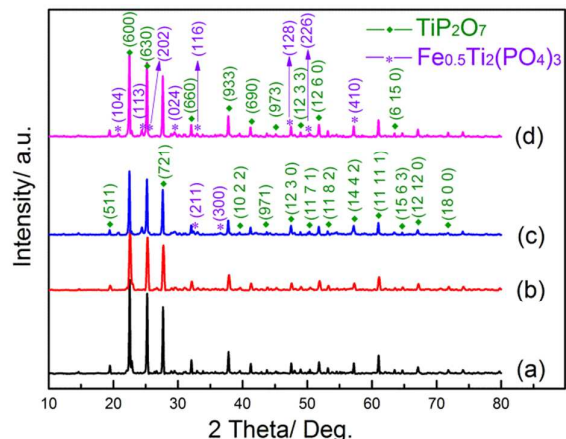


Fig. 1 XRD patterns of (a) bared, (b) carbon coated, (c) ITP coated and (d) carbon-ITP coated  $\text{TiP}_2\text{O}_7$ .

Fig. 1 shows the X-ray diffraction patterns of as-prepared samples. It is clear in Fig. 1 (a) and (b) that the bared and the carbon-coated  $\text{TiP}_2\text{O}_7$  are similar, which indicates that carbon is in amorphous state and carbon-coating has no influence on the crystal lattice of the host. Fig. 1 (c) shows that  $\text{TiP}_2\text{O}_7$  is the

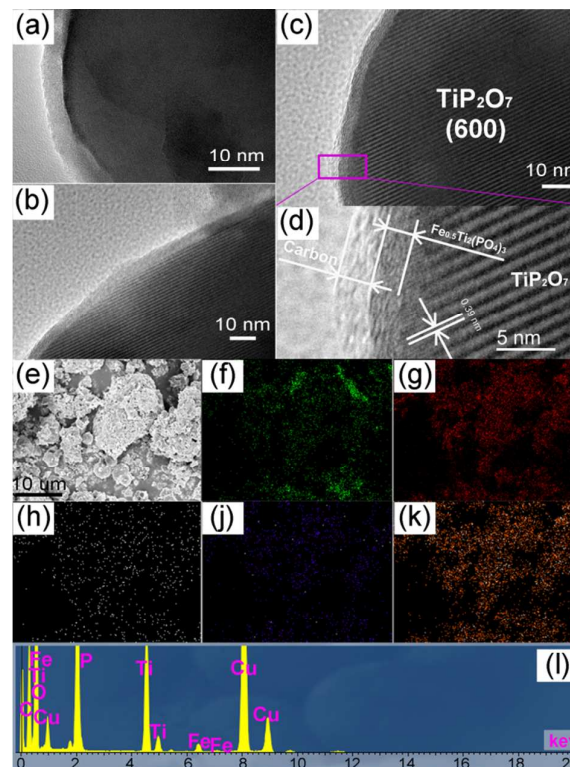


Fig. 2 HRTEM of (a) carbon coated, (b) ITP coated, (c) carbon-ITP coated  $\text{TiP}_2\text{O}_7$  and (d) the detail of the carbon-ITP coated  $\text{TiP}_2\text{O}_7$ , and (e) FESEM image with elemental maps of (f) C, (g) O, (h) P, (j) Fe and (k) Ti, respectively, and (l) TEM-EDX of the carbon-ITP coated sample.

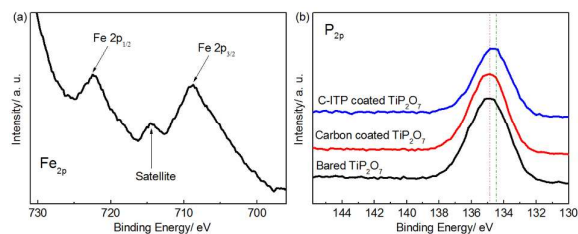


Fig. 3 XPS spectra of (a) Fe in the carbon-ITP coated  $\text{TiP}_2\text{O}_7$  and (b) P in the bared, carbon coated and carbon-ITP coated  $\text{TiP}_2\text{O}_7$ , respectively.

major constituent. In addition, a second phase is observed which is in agreement with the presence of the ITP phase.<sup>38</sup> Fig. 1 (d) is consistent with Fig. 1 (c). The two samples both suggest that ITP phase has no influence on the crystal lattice of the host, which indicates the possibility of the ITP phase acting as a coating layer. Fig. S2 and Fig. S3 further shows that with the increase of the content of the  $\text{FeC}_2\text{O}_4$  precursor, a progressive increase of the contribution of the ITP phase is observed, indicating that two phases remain in separation, and the ITP phase along with the carbon coated layer should be on the surface of the  $\text{TiP}_2\text{O}_7$  host rather than in the crystal lattice of the matrix. Morphologies in Fig. 2 validate this pattern.

Fig. 2 (a) and (b) is the HRTEM of carbon-coated and ITP-coated  $\text{TiP}_2\text{O}_7$ , respectively. Both of the samples are well crystallized in the hosts with the matrices being well covered with a clearly visible mono-layer. The carbon-coated  $\text{TiP}_2\text{O}_7$  particle has a relatively rough surface, which differs from the smooth surface of the ITP-coated particle (Fig. S4). Furthermore, the ITP layer seems to be closer to the host than the carbon layer. This is because the ITP phase is generated by the reaction between  $\text{FeC}_2\text{O}_4$  and the  $\text{TiP}_2\text{O}_7$  matrix and thereby fits the matrix well more than the carbon phase. As a result, the ITP phase and the  $\text{TiP}_2\text{O}_7$  matrix tend to be melted with each other. In the case of the carbon-ITP coated  $\text{TiP}_2\text{O}_7$ , as shown in Fig. 2 (c) and (d), a bi-layer coater can be easily identified which is tightly covered on the interference fringes of the matrix. With the aid of the details of the Moire fringes shown in Fig. 2 (d), the facet can be determined to agree well to (6 0 0) of the  $\text{TiP}_2\text{O}_7$  matrix. According to the differences of the carbon and ITP phase shown in Fig. 2 (a) and (b), the outer coater in the bi-layer in Fig. 2 (c) can be ascribed to the carbon, and the inner layer agrees to the ITP phase. Fig. S5 shows that the ITP layer is crystallized with its lattice (113) facing to (630) of the  $\text{TiP}_2\text{O}_7$  matrix, which certifies the identification between the TEM and the XRD.

The carbon-ITP coated sample was subjected to TG in order to determine the mass ratio of carbon layer (Fig. S6). As a result, the weight loss is about 3.5 wt %, indicating a thin carbon layer, which is in accordance with the HRTEM in Fig. 2 (c) and (d). Fig. 2 (e) shows the area of energy dispersive X-ray (EDX) analysis of the sample. The elemental maps of C, O, P, Fe and Ti were explored in this area, as displayed in Fig. 2 (f)–(k). These maps illustrate the outlines of the particles. The distribution of C and Fe is in accordance with other elements. This result is in agreement with the HRTEM shown in Fig. 2 (c) and (d). The EDX carried out with TEM is also collected as shown in Fig. 2 (l), which confirms this result.

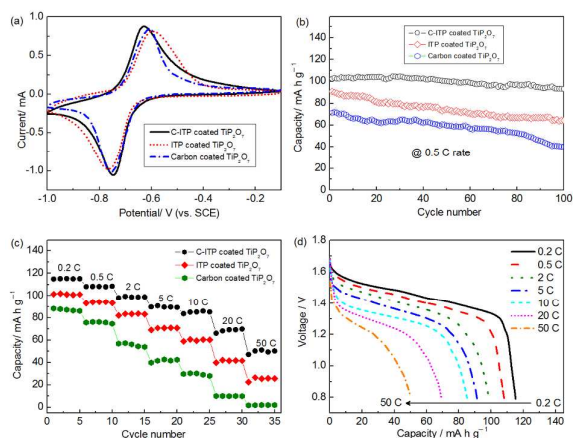


Fig. 4 Electrochemical performances of the carbon coated, ITP coated and carbon-ITP coated  $\text{TiP}_2\text{O}_7$ . (a) CV curves carried out at a scan rate of  $0.5 \text{ mV s}^{-1}$ , (b) cycling performances at a current rate of 0.5 C, (c) rate performances from 0.2 C to 50 C and (d) the discharge curves of the full cell with carbon-ITP coated  $\text{TiP}_2\text{O}_7$  as the anode at various rates.

In order to further certify the content of the inner layer, XPS for the carbon-ITP coated sample was carried out and shown in Fig. 3 (a), which determines that the element Fe has a valence of 2. The binding energy peak centred at 708.9 and 722.5 eV belongs to  $\text{Fe } 2p_{3/2}$  and  $\text{Fe } 2p_{1/2}$ , respectively. The satellite peak for  $\text{Fe } 2p_{3/2}$  was observed at 714.8 eV. The binding energy difference between the  $\text{Fe } 2p_{3/2}$  peak and the satellite peak is approximately 6 eV. These results present a clear evidence for the existence of  $\text{Fe}^{2+}$ .<sup>39–41</sup> Fig. 3 (b) validates the existence of  $(\text{PO}_4)^{3-}$ .<sup>23</sup> The peaks of phosphorus for the bared and carbon-coated  $\text{TiP}_2\text{O}_7$  are centered at the same location while the corresponding peak for carbon-ITP coated  $\text{TiP}_2\text{O}_7$  moves to a lower binding energy. This result agrees to the presence of the  $(\text{PO}_4)^{3-}$ , in which phosphorus has lower binding energy than in  $\text{TiP}_2\text{O}_7$ .<sup>42</sup> These results clearly show that the inner layer is composed of ITP phase.

Fig. 4 gives the electrochemical performances of the carbon coated, ITP coated and the carbon-ITP coated samples. CV curves carried out in 1 M  $\text{Li}_2\text{SO}_4$  aqueous electrolyte are shown in Fig. 4 (a). All three samples obtain one pair of symmetric redox peaks at a low coating mass. The distance between the oxidation peak and the reduction peak is reduced for the carbon-ITP coated sample which indicates that the electrochemical reversibility was elevated after the carbon-ITP treatment.<sup>43</sup> In an aqueous system, the voltage platform difference between charge and discharge is usually not small. On the one hand, the charged electrode is more active than the discharged electrode. On the other hand, aqueous solutions are more corrosive than organic electrolyte. The cooperation of the two factors makes the charged electrode be vulnerable to aqueous attack with a higher exchange current density. As a result, the potential difference between the charge and discharge of the aqueous battery is increased. A protective coater is thereby necessary, while a conductive

coater is more favourable which can effectively reduce the difference and benefit a longer cycle life and a higher charge-discharge rate.

Cycling performances at a rate of 0.5 C for the three samples in  $\text{TiP}_2\text{O}_7$ |aqueous  $\text{Li}_2\text{SO}_4$ | $\text{LiMn}_2\text{O}_4$  full cells are given in Fig. 4 (b). The carbon-ITP coated  $\text{TiP}_2\text{O}_7$  delivers a higher discharge capacity as well as better stability than the other samples. It has been suggested that the capacity fading is related to such factors as transition metal ion dissolution, phase transformation, and decomposition of the electrolyte.<sup>44–46</sup> The XRD patterns of carbon-coated  $\text{TiP}_2\text{O}_7$  and carbon-ITP coated  $\text{TiP}_2\text{O}_7$  before and after 100 cycles are compared carefully (Fig. S7). For the carbon-coated sample, a distortion can be observed in the patterns, though the main structure of  $\text{TiP}_2\text{O}_7$  is maintained after 100 cycles. It is believed that this kind of phase transformation is related to the formation of new compounds.<sup>47–49</sup> In the case of the carbon-ITP coated  $\text{TiP}_2\text{O}_7$  sample, little variation for the positions and outlines of the peaks in the XRD pattern is observed. It indicates that the anode is stable. Fig. 4 (c) presents the rate performance at 0.2–50 C (1 C = 100 mA g<sup>-1</sup>) in the electrochemical window of 0.8–1.7 V at room temperature for the three samples. The carbon-ITP sample exhibits a better rate performance with a discharge capacity of 69.8 mA h g<sup>-1</sup> and 51.2 mA h g<sup>-1</sup> delivered at a rate of 20 C and 50 C, respectively. In the case of the carbon coated and ITP coated samples, discharge capacities are greatly reduced at the same rate. The discharge curves of the carbon-ITP coated  $\text{TiP}_2\text{O}_7$  at various rates after a full charge at 0.2 C rate are shown in Fig. 4 (d). It can be seen that all of the discharge curves obtain obvious plateaus. At the rate of 0.2 C, the sample exhibits a capacity of 115 mA h g<sup>-1</sup>, which is one of the best results we have known. According to this result, the  $\text{TiP}_2\text{O}_7$ |aqueous  $\text{Li}_2\text{SO}_4$ | $\text{LiMn}_2\text{O}_4$  full cell can obtain an expected energy density of 84.3 W h kg<sup>-1</sup>, which is much higher than lead-acid battery.

The result indicates that the ITP layer might contribute to the capacity. According to the CV curve of the carbon-ITP coated sample prepared at an elevated ratio of Fe precursor, a double pair of redox peaks appears which suggests that the ITP layer exhibits electrochemical activity and elevates the capacity of the sample (Fig. S9). The carbon-ITP coated  $\text{TiP}_2\text{O}_7$  delivers a high discharge capacity of 81.2 mA h g<sup>-1</sup> and exhibits excellent cycling performance with less than 25% capacity loss over 800 cycles at a 10 C charge/discharge rate (Fig. S10). These results prove that the carbon-ITP coated  $\text{TiP}_2\text{O}_7$  is suitable for a high-performance aqueous lithium battery.

In summary, we successfully fabricated a carbon-ITP phase separated conducting bi-layer on the surface of the  $\text{TiP}_2\text{O}_7$  anode material for the aqueous lithium battery. Compared with the mono-layer of carbon or ITP-coated  $\text{TiP}_2\text{O}_7$ , the double-layered sample delivers a higher discharge capacity of 115 mA h g<sup>-1</sup> at 0.2 C rate and exhibits elevated rate performance with less than 25% capacity loss over 800 cycles at a 10 C charge/discharge rate. It obtains a capacity of 51.2 mA h g<sup>-1</sup> at 50 C in a  $\text{TiP}_2\text{O}_7$ |aqueous  $\text{Li}_2\text{SO}_4$ | $\text{LiMn}_2\text{O}_4$  full cell as well. It is speculated that the enhanced performance could be

ascribed to the well-constructed electron-ion phase-separated conducting layer.

## Acknowledge

National Natural Science Foundation of China (51273027), the Priority Academic Program Development of Jiangsu Higher Education Institutions (PAPD) and Jiangsu Key Laboratory of Advanced Catalytic Materials and Technology (BM2012110) and Advanced Catalysis and Green Manufacturing Collaborative Innovation Center, Changzhou University are gratefully acknowledged.

## Notes and references

Jiangsu Key Laboratory of Advanced Catalytic materials and technology, Changzhou University, Changzhou, China. \*E-mail: jinhongshi0001@163.com

†Electronic Supplementary Information (ESI) available. See DOI: 10.1039/x0xx00000x

‡ Equal contribution to this work.

- 1 T. Zhang and H. Zhou, *Nat. Commun.*, 2013, 4, 1817.
- 2 T. Zhang and H. Zhou, *Angew. Chem., Int. Ed.*, 2012, 51, 11062.
- 3 B. Zhang, Y. Liu, X. Wu, Y. Yang, Z. Chang, Z. Wen and Y. Wu, *Chem. Commun.*, 2014, 50, 1209.
- 4 Y. Liu, Z. Wen, X. Wu, X. Wang, Y. Wu and R. Holze, *Chem. Commun.*, 2014, 50, 13714.
- 5 X. Wang, Q. Qu, Y. Hou, F. Wang and Y. Wu, *Chem. Commun.*, 2013, 49, 6179.
- 6 G. Wang, L. Fu, N. Zhao, L. Yang, Y. Wu and H. Wu, *Angew. Chem., Int. Ed.*, 2007, 46, 295.
- 7 Q. Qu, Y. Zhu, X. Gao and Y. Wu, *Adv. Energy Mater.* 2012, 2(8), 950.
- 8 Z. Wan, J. Shao, J. Yun, H. Zheng, T. Gao, M. Shen, Q. Qu and H. Zheng, *Small*, 2014, 10,( 23), 4975.
- 9 X. Zhou, Z. Dai, S. Liu, J. Bao and Y. Guo, *Adv. Mater.*, 2014, 26(23), 3943.
- 10 F. Zhao, B. Wang, Y. Tang, H. Ge, Z. Huang and H. Liu, *J. Mater. Chem. A*, 2015, 3(45), 22969.
- 11 L. Liu, H. Zhang, J. Yang, Y. Mu and Y. Wang, *Chem.-A Europ. J.*, 2015, 21(52), 19104.
- 12 Q. Jiang, D. Liu, H. Zhang and S. Wang, *J. Phys. Chem. C*, 2015, 119(52), 28776.
- 13 W. Wu, S. Shanbhag, A. Wise, J. Chang, A. Rutt and J. F. Whitacre, *J. Electrochem. Soc.*, 2015, 162(9), A1921.
- 14 K. Bazzi, M. Nazri, V. M. Naik, V. K. Garg, A. C. Oliveira, P. P. Vaishnava, G. A. Nazri and R. Naik, *J. Power Sources*, 2016, 306, 17.
- 15 Z. Guo, D. Zhang, H. Qiu, Y. Ju, T. Zhang, L. Zhang, Y. Meng, Y. Wei and G. Chen, *RSC Adv.*, 2016, 6(8), 6523.
- 16 L. Zhang, J. M. Tarascon, M. T. Sougrati, G. Rousse and G. Chen, *J. Mater. Chem. A*, 2015, 3(33), 16988.
- 17 H. Liu, W. Li, D. Shen, D. Zhao and G. Wang, *J. Am. Chem. Soc.*, 2015, 137 (40), 13161.
- 18 P. Hovington, M. Lagacé, A. Guerfi, P. Bouchard, A. Mauger, C. M. Julien, M. Armand and K. Zaghib, *Nano Lett.*, 2015, 15 (4), 2671.
- 19 C. Y. Wu, G. S. Cao, H. M. Yu, J. Xie and X. B. Zhao, *J. Phys. Chem. C*, 2011, 115 (46), 23090.
- 20 Q. Liu, H. He, Z. Li, Y. Liu, Y. Ren, W. Lu, J. Lu, E. A. Stach and J. Xie, *ACS Appl. Mater. Interfaces*, 2014, 6 (5), 3282.

- 21 A. Nie, L. Gan, Y. Cheng, Q. Li, Y. Yuan, F. Mashayek, H. Wang, R. Klie, U. Schwingenschlogl and R. S. Yassar, *Nano Lett.*, 2015, 15 (1), 610.
- 22 N. R. McLaren, R. I. Smith and A. R. West, *Chem. Mater.*, 2011, 23 (15), 3556.
- 23 B. Kang and G. Ceder, *nature*, 2009, 458, 190.
- 24 K. Zaghib, J. B. Goodenough, A. Mauger and C. Julien, *J. Power Sources*, 2009, 194(2), 1021.
- 25 G. Ceder and B. Kang, *J. Power Sources*, 2009, 194(2), 1024.
- 26 Y. Cho, P. Oh and J. Cho, *Nano Lett.*, 2013, 13, 1145.
- 27 J. Lu, Q. Peng, W. Wang, C. Nan, L. Li and Y. Li, *J. Am. Chem. Soc.* 2013, 135, 1649.
- 28 L. Peng, H. Zhang, L. Fang, Y. Zhang and Y. Wang, *Nanoscale* 2016, 8(4), 2030.
- 29 L. Shen, E. Uchaker, X. Zhang and G. Cao, *Adv. Mater.*, 2012, 24 (48), 6502.
- 30 A. K. Rai, J. Gim, J. Song, V. Mathew, L. T. Anh and J. Kim, *Electrochim. Acta*, 2012, 75, 247.
- 31 Z. Shi, Q. Wang, W. Ye, Y. Li and Y. Yang, *Micropor. Mesopor. Mater.*, 2006, 88, 232.
- 32 S. Patoux and C. Masquelier, *Chem. Mater.* 2002, 14, 5057.
- 33 V. Aravindan, M. V. Reddy, S. Madhavi, S. G. Mhaisalkar, G. V. Subba Rao and B. V. R. Chowdari, *J. Power Sources*, 2011, 196, 8850.
- 34 A. K. Rai, J. Lim, V. Mathew, J. Gim, J. W. Kang and J. K. Kim, *Electrochem. Commun.*, 2012, 19, 9.
- 35 H. Wang, K. Huang, Y. Zeng, S. Yang and L. Chen, *Electrochim. Acta.*, 2007, 52, 3280.
- 36 V. Nalini, M. H. Sorby, K. Ameszawa, R. Haugsrud, H. Fjellvag and T. Norby, *J. Am. Ceram. Soc.*, 2011, 94(5), 1514.
- 37 C. Li, X. Sun, Q. Du and H. Zhang, *Solid State Ionics*, 2013, 249–250, 72.
- 38 S. Benmokhtar, A. E. Jazouli, A. Aatiqa, J. P. Chaminade, P. Gravereaub, A. Wattiauxb, L. Fournes and J. C. Grenier, *Solid State Ionics* 2007, 180, 2004.
- 39 S. J. Roosendaal, B. van Asselen, J. W. Elsenaar, A. M. Vredenberg and F. H. P. M. Habraken, *Surf. Sci.* 1999, 442, 329.
- 40 P. C. J. Graat and M. A. J. Somers, *Appl. Surf. Sci.* 1996, 100, 36.
- 41 T. Yamashita and P. Hayes, *Appl. Surf. Sci.* 2008, 254, 2441.
- 42 W. E. Morgan, W. J. Stec and J. R. Vanwazer, *J. Am. Chem. Soc.* 1973, 95, 751.
- 43 S. Y. Chen, C. H. Mi, L. H. Su, B. Gao, Q. B. Fu and X. G. Zhang, *J. Appl. Electrochem.*, 2009, 39, 1943.
- 44 W. Li and J. R. Dahn, *J. Electrochem. Soc.* 1995, 142, 1742.
- 45 W. Li, W. R. Mckinno and J. R. Dahn, *J. Electrochem. Soc.* 1994, 141, 2310.
- 46 M. Zhang and J. R. Dahn, *J. Electrochem. Soc.* 1996, 143, 2730.
- 47 W. Tang, S. Tian, L. Liu, L. Li, H. P. Zhang, Y. B. Yue, Y. Bai, Y. P. Wu and K. Zhu, *Electrochem. Commun.*, 2011, 13, 205.
- 48 S. Zheng, P. Han, Z. Han, P. Li, H. Zhang and J. Yang, *Adv. Energy Mater.*, 2014, 4, 1400226.
- 49 W. Tang, Y. Zhu, Y. Hou, L. Liu, Y. Wu, K. P. Loh, H. Zhang and K. Zhu, *Energy Environ. Sci.*, 2013, 6, 2093.

**Graphical Abstract**

A phase separation of the electron-ion conducting layer on the surface of  $\text{TiP}_2\text{O}_7$  anode material greatly elevates the electrochemical performances.

